Available online at www.sciencedirect.com
ScienceDirect
Information Sciences 177 (2007) 360–377
INFORMATION SCIENCES
AN INTERNATIONAL JOURNAL
www.elsevier.com/locate/ins

New results about the centroid of an interval type-2 fuzzy set, including the centroid of a fuzzy granule

Jerry M. Mendel [a,*], Hongwei Wu [b,c]

[a] *Signal and Image Processing Institute, Department of Electrical Engineering, University of Southern California, 3740 McClintock Avenue, Los Angeles, CA 90089-2564, United States*
[b] *Computational Biology Institute, Oak Ridge National Laboratory, Oak Ridge, TN 37831, United States*
[c] *Computational Systems Biology Laboratory, Department of Biochemistry and Molecular Biology, University of Georgia, Athens, GA 30602, United States*

Abstract

The centroid of an interval type-2 fuzzy set (IT2 FS) provides a measure of the uncertainty of such a FS. Its calculation is very widely used in interval type-2 fuzzy logic systems. In this paper, we present properties about the centroid of an IT2 FS. We also illustrate many of the general results for a T2 fuzzy granule (FG) in order to develop some understanding about the uncertainty of the FG in terms of its vertical and horizontal dimensions. At present, the T2 FG is the only IT2 FS for which it is possible to obtain closed-form formulas for the centroid, and those formulas are in this paper.

Keywords: Centroid; Centroid properties; Interval type-2 fuzzy set; Type-2 fuzzy set; Fuzzy granule

1. Introduction

An interval type-2 fuzzy set (IT2 FS) is today the most widely used T2 FS because it is computationally simple to use. When such FSs are used in a rule-based fuzzy logic system (FLS) (e.g., [1,2,5–10,12,13,20,22]), the result is an interval T2 FLS (IT2 FLS). In such a FLS, fired-rule output sets are also IT2 FSs, and to go from such sets to a number, as is usually required in most engineering applications of a FLS, one must perform two successive operations, type-reduction and defuzzification. Type-reduction maps the output T2 FS into a type-1 (T1) FS, and defuzzification converts that T1 FS into a number.

Type-reduction methods were developed by Karnik and Mendel [3,4] and are elaborated upon in [12]. When they are applied to a general T2 FS they require an astronomical number of computations. When they are applied to an IT2 FS, they require a very small number of computations, which is one of the major reasons that IT2 FLSs have received attention whereas general T2 FLSs have not.

* Corresponding author. Tel.: +1 213 740 4445; fax: +1 213 740 4651.
E-mail addresses: mendel@sipi.usc.edu (J.M. Mendel), hongweiw@csbl.bmb.uga.edu (H. Wu).

0020-0255/$ - see front matter
doi:10.1016/j.ins.2006.03.003

Even for IT2 FLSs there can be many different kinds of type-reduction. The ones that have been developed so far all extend a T1 centroid calculation to T2 FSs, so that if all sources of uncertainty disappear the output of an IT2 FLS reduces to that of a T1 FLS. So, computing the centroid of an IT2 FS plays a central role in IT2 FLSs.

The centroid of an IT2 FS also provides a measure of the uncertainty of an IT2 FS [21], and more recently has been the basis for going from data collected from a group of subjects (about an interval that they associate with the meaning of a word) to the footprint of uncertainty (FOU) of an IT2 FS that models that word [17].

In this paper, we present properties about the centroid of an IT2 FS. We also provide a formula for the centroid of an IT2 fuzzy granule (FG), one that lets us develop some understanding about the uncertainty of the FG in terms of its vertical and horizontal dimensions. To begin, we briefly review IT2 FSs and the centroid of such FSs.

2. Basics of an interval type-2 fuzzy set

An *interval T2 FS* $\widetilde{A}$ is characterized as[1] [12,16]

$$\widetilde{A} = \int_{x\in X}\int_{u\in J_x\subseteq[0,1]} 1/(x,u) = \int_{x\in X}\left[\int_{u\in J_x\subseteq[0,1]} 1/u\right]\Big/x \tag{1}$$

where x, the *primary variable*, has domain X; u, the *secondary variable*, has domain J_x at each $x\in X$; J_x is called the *primary membership* of x; and, the *secondary grades* of $\widetilde{A}$ all[2] equal 1. Uncertainty about $\widetilde{A}$ is conveyed by the union of all of the primary memberships, which is called the *footprint of uncertainty* (FOU) of $\widetilde{A}$, i.e.

$$\mathrm{FOU}(\widetilde{A}) = \bigcup_{x\in X} J_x \tag{2}$$

The upper membership function (UMF) and lower membership function (LMF) of $\widetilde{A}$ are two type-1 MFs that bound the FOU (e.g., see Fig. 1). The UMF is associated with the upper bound of $\mathrm{FOU}(\widetilde{A})$ and is denoted $\bar{\mu}_{\widetilde{A}}(x),\ \forall x\in X$, and the LMF is associated with the lower bound of $\mathrm{FOU}(\widetilde{A})$ and is denoted $\underline{\mu}_{\widetilde{A}}(x)$, $\forall x\in X$, i.e.

$$\bar{\mu}_{\widetilde{A}}(x) \equiv \overline{\mathrm{FOU}(\widetilde{A})} \quad \forall x\in X \tag{3}$$

$$\underline{\mu}_{\widetilde{A}}(x) \equiv \underline{\mathrm{FOU}(\widetilde{A})} \quad \forall x\in X \tag{4}$$

Note that

$$J_x = \left[\underline{\mu}_{\widetilde{A}}(x), \bar{\mu}_{\widetilde{A}}(x)\right] \tag{5}$$

so that $\mathrm{FOU}(\widetilde{A})$ in (2) can also be expressed as

$$\mathrm{FOU}(\widetilde{A}) = \bigcup_{x\in X}\left[\underline{\mu}_{\widetilde{A}}(x), \bar{\mu}_{\widetilde{A}}(x)\right] \tag{6}$$

For continuous universes of discourse X and U, an *embedded interval T2 FS* $\widetilde{A}_e$ is

$$\widetilde{A}_e = \int_{x\in X}[1/\theta]/x \quad \theta\in J_x\subseteq U=[0,1] \tag{7}$$

Set $\widetilde{A}_e$ is embedded in $\widetilde{A}$ such that at each x it only has one secondary variable (Fig. 1, where secondary grades, not shown, are all equal to 1). Although there are an uncountable number of embedded IT2 FSs, such FSs are still quite useful in theoretical developments. Other examples of $\widetilde{A}_e$ are $1/\bar{\mu}_{\widetilde{A}}(x)$ and $1/\underline{\mu}_{\widetilde{A}}(x)$, $\forall x\in X$.

[1] We shall inter-twine our discussions about fuzzy sets that are defined on continuous or discrete universes of discourse. For discrete universes of discourse, one should replace the integral signs (e.g., in (1)) with summation signs. Regardless of which notation is used, each symbol represents the set-theoretic union operation.

[2] In a general T2 FS, the secondary grades can take on any value in $[0,1]$.

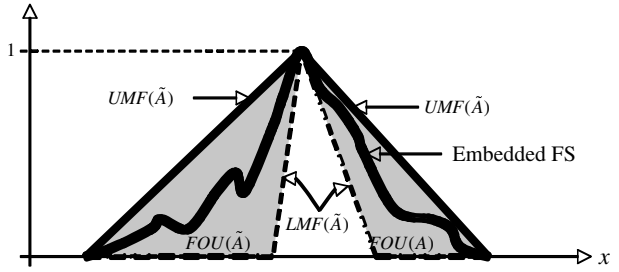

Fig. 1. FOU (shaded), LMF (dashed), UMF (solid) and an embedded FS (wavy line) for IT2 FS $\widetilde{A}$.

Associated with each $\widetilde{A}_e$ is an *embedded T1 FS* A_e, where

$$A_e = \int_{x\in X} \theta/x \quad \theta \in J_x \subseteq U = [0,1] \tag{8}$$

Set A_e is the union of all the primary memberships of the set $\widetilde{A}_e$ in (7) (Fig. 1), and there are an uncountable number of A_e. Other examples of A_e are $\bar{\mu}_{\tilde{A}}(x)$ and $\underline{\mu}_{\tilde{A}}(x)$, $\forall x \in X$. Note that A_e acts as the domain for $\widetilde{A}_e$.

For discrete universes of discourse, in which both the primary and secondary variables[3] are discretized, there exist a countable number of embedded T2 (and T1) FSs (e.g., see [16] or [12]). In this case, $\widetilde{A}_e$ and A_e are given by formulas like (12) and (15) below.

A *symmetric* IT2 FS is a special case of an IT2 FS, and is one for which the FOU is symmetrical about $x = m$, i.e.

$$\bar{\mu}_{\tilde{A}}(m+x) = \bar{\mu}_{\tilde{A}}(m-x) \tag{9}$$

$$\underline{\mu}_{\tilde{A}}(m+x) = \underline{\mu}_{\tilde{A}}(m-x) \tag{10}$$

In [16] a new *Representation Theorem* was derived in which a general T2 FS, $\widetilde{A}$, is expressed as the union of all of its embedded T2 FSs, $\widetilde{A}_e^j$. For an IT2 FS, for which X and U are discrete, this can be stated as

$$\widetilde{A} = \sum_{j=1}^{n_A} \widetilde{A}_e^j \tag{11}$$

where

$$\widetilde{A}_e^j = \sum_{i=1}^{N} [1/u_i^j]/x_i \quad u_i^j \in J_{x_i} \subseteq U = [0,1] \tag{12}$$

and

$$n_A = \prod_{i=1}^{N} M_i \tag{13}$$

in which M_i denotes the discretization levels of secondary variable u_i^j at each of the N x_i. Because all of the secondary grades of an IT2 FS equal 1, we can also express (11) and (12) as

$$\widetilde{A} = 1/\mathrm{FOU}(\widetilde{A}) = 1 \Big/ \sum_{j=1}^{n_A} A_e^j \tag{14}$$

where

$$A_e^j = \sum_{i=1}^{N} u_i^j \Big/ x_i \quad u_i^j \in J_{x_i} \subseteq U = [0,1] \tag{15}$$

[3] Strictly speaking, a T2 FS whose secondary variable is discrete is not an IT2 FS, because an IT2 FS requires that the domain for the secondary variable must be an interval. It is usually for computational purposes that we discretize the secondary variable.

and it is understood that the notation in (14) means that the secondary grade equals 1 at all elements in $\mathrm{FOU}(\widetilde{A})$.

With reference to Fig. 1, (14) means collecting all embedded IT2 FSs into a *bundle* of such sets. This bundle will always be bounded by the UMF and the LMF of the FOU, since they are both legitimate embedded sets.

3. Centroid of an interval type-2 fuzzy set

Using the Representation Theorem in (11), we define the centroid, $C_{\widetilde{A}}$, of an IT2 FS $\widetilde{A}$ as the collection of the centroids of all of its embedded IT2 FSs. From (14), we see that this means we need to compute the centroids of all of the n_A embedded T1 FSs contained within $\mathrm{FOU}(\widetilde{A})$. The results of doing this will be a collection of n_A numbers, and these numbers will have both a smallest and largest element, $c_l(\widetilde{A}) \equiv c_l$ and $c_r(\widetilde{A}) \equiv c_r$, respectively. That such numbers exist is because the centroid of each of the embedded T1 FSs is a bounded number. Associated with each of these numbers will be a membership grade of 1, because the secondary grades of an IT2 FS are all equal to 1. This means

$$C_{\widetilde{A}} = 1/\{c_l, \ldots, c_r\} \tag{16}$$

where[4]

$$c_l = \min_{\forall \theta_i \in [\underline{\mu}_{\widetilde{A}}(x_i), \bar{\mu}_{\widetilde{A}}(x_i)]} \frac{\sum_{i=1}^{N} x_i \theta_i}{\sum_{i=1}^{N} \theta_i} \tag{17}$$

$$c_r = \max_{\forall \theta_i \in [\underline{\mu}_{\widetilde{A}}(x_i), \bar{\mu}_{\widetilde{A}}(x_i)]} \frac{\sum_{i=1}^{N} x_i \theta_i}{\sum_{i=1}^{N} \theta_i} \tag{18}$$

and

$$x_1 < x_2 < \cdots < x_N \tag{19}$$

The latter is true because x_i are sampled values of the primary variable; x_1 denotes the left-hand (smallest) sampled value and x_N denotes the right-hand (largest) sampled value.[5]

Except for one very special FOU, an interval T2 fuzzy granule, which we shall examine in Section 6, there are no known closed-form formulas for c_l and c_r; however, Karnik and Mendel [3,4] have developed iterative algorithms for computing these end-points exactly. Because their published algorithms are contained within more general algorithms for the case when both x_i and θ_i vary over intervals [for which (17) and (18) must also include the variations of each of the x_i, and one is then led to a[6] *generalized centroid*], we include statements of the two algorithms for computing c_l and c_r in Appendix A. Here we establish the bases for computing c_l and c_r using (17) and (18). Our presentation follows that of [12].

If we take the usual calculus approach to optimizing $y(\theta_1, \ldots, \theta_N) = \sum_{i=1}^{N} x_i \theta_i / \sum_{i=1}^{N} \theta_i$, and differentiate $y(\theta_1, \ldots, \theta_N)$ with respect to θ_k, we find that:

$$\frac{\partial y(\theta_1, \ldots, \theta_N)}{\partial \theta_k} = \frac{\partial}{\partial \theta_k}\left[\frac{\sum_{i=1}^{N} x_i \theta_i}{\sum_{i=1}^{N} \theta_i}\right] = \frac{x_k - y(\theta_1, \ldots, \theta_N)}{\sum_{i=1}^{N} \theta_i} \tag{20}$$

Because $\sum_{i=1}^{N} \theta_i > 0$, it is easy to see from (20) that

$$\frac{\partial y(\theta_1, \ldots, \theta_N)}{\partial \theta_k} \begin{cases} \geqslant 0 & \text{if } x_k \geqslant y(\theta_1, \ldots, \theta_N) \\ < 0 & \text{if } x_k < y(\theta_1, \ldots, \theta_N) \end{cases} \tag{21}$$

[4] When discretizations of the primary variable and primary membership approach zero, $\{c_l, \ldots, c_r\} \to [c_l, c_r]$, an interval set. In the literature about the centroid, it is customary to see (16) written as $C_{\widetilde{A}} = [c_l, c_r]$.

[5] If Gaussian MFs are used, then in theory $x_1 \to -\infty$ and $x_N \to \infty$; but, in practice when truncations are used x_1 and x_N are again finite numbers.

[6] The so-called *fuzzy weighted average* (e.g., [11]) is a generalized centroid in which x_i and θ_i are both general fuzzy numbers. Equations analogous to (17) and (18) were also obtained in [11].

Unfortunately, equating $\partial y/\partial\theta_k$ to zero does not give us any information about the value of θ_k that optimizes $y(\theta_1,\ldots,\theta_N)$. When we do this we find:

$$y(\theta_1,\ldots,\theta_N)=x_k \Rightarrow \frac{\sum_{i=1}^{N}x_i\theta_i}{\sum_{i=1}^{N}\theta_i}=x_k \Rightarrow \frac{\sum_{i\neq k}^{N}x_i\theta_i}{\sum_{i\neq k}^{N}\theta_i}=x_k \tag{22}$$

Observe that θ_k no longer appears in the final expression in (22), so that the direct calculus approach does not work.

Eq. (21) does give the direction in which θ_k should be changed in order to increase or decrease $y(\theta_1,\ldots,\theta_N)$, i.e.

$$\left.\begin{array}{ll}\text{If } x_k > y(\theta_1,\ldots,\theta_N) & y(\theta_1,\ldots,\theta_N) \text{ increases (decreases) as } \theta_k \text{ increases (decreases)}\\ \text{If } x_k < y(\theta_1,\ldots,\theta_N) & y(\theta_1,\ldots,\theta_N) \text{ increases (decreases) as } \theta_k \text{ decreases (increases)}\end{array}\right\} \tag{23}$$

Recall (see (17) and (18)) that the maximum value that θ_k can attain is $\bar{\mu}_{\tilde{A}}(x_k)$ and the minimum value that it can attain is $\underline{\mu}_{\tilde{A}}(x)$. Eq. (23) therefore implies that $y(\theta_1,\ldots,\theta_N)$ attains its *maximum value*, c_r, if:

1. $\theta_k=\bar{\mu}_{\tilde{A}}(x_k)\ \forall k \ni x_k > y(\theta_1,\ldots,\theta_N)$,
2. $\theta_k=\underline{\mu}_{\tilde{A}}(x)\ \forall k \ni x_k < y(\theta_1,\ldots,\theta_N)$.

Similarly, we can deduce from (23) that $y(\theta_1,\ldots,\theta_N)$ attains its *minimum value*, c_l, if:

1. $\theta_k=\bar{\mu}_{\tilde{A}}(x_k)\ \forall k \ni x_k < y(\theta_1,\ldots,\theta_N)$,
2. $\theta_k=\underline{\mu}_{\tilde{A}}(x)\ \forall k \ni x_k > y(\theta_1,\ldots,\theta_N)$.

Note also that because $\theta_k \geqslant 0$ for all k, the partial derivative $\partial y/\partial x_k=\theta_k/\sum_{i=1}^{N}\theta_i \geqslant 0$. Therefore, y is non-decreasing (non-increasing) with increasing (decreasing) x_k. Combining this fact with the two possible choices for θ_k that are stated above, we see that to compute $c_r(c_l)$ θ_k *switches only one time* between $\bar{\mu}_{\tilde{A}}(x_k)$ and $\underline{\mu}_{\tilde{A}}(x)$. The Karnik–Mendel algorithms locate the switch point, and in general the switch point for c_r, R, is different from the switch point for c_l, L.

Putting all of these facts together, we obtain the following formulas for c_l and c_r:

$$c_l=\frac{\sum_{i=1}^{L}x_i\bar{\mu}_{\tilde{A}}(x_i)+\sum_{i=L+1}^{N}x_i\underline{\mu}_{\tilde{A}}(x_i)}{\sum_{i=1}^{L}\bar{\mu}_{\tilde{A}}(x_i)+\sum_{i=L+1}^{N}\underline{\mu}_{\tilde{A}}(x_i)} \tag{24}$$

$$c_r=\frac{\sum_{i=1}^{R}x_i\underline{\mu}_{\tilde{A}}(x_i)+\sum_{i=R+1}^{N}x_i\bar{\mu}_{\tilde{A}}(x_i)}{\sum_{i=1}^{R}\underline{\mu}_{\tilde{A}}(x_i)+\sum_{i=R+1}^{N}\bar{\mu}_{\tilde{A}}(x_i)} \tag{25}$$

Another way to summarize these results, that we will make use of in the sequel, is to state them for continuous universes of discourse. Let $A_e(l)$ denote an embedded T1 FS for which (in the sequel, we sometimes let $\bar{\mu}(x)$ and $\underline{\mu}(x)$ be short for $\bar{\mu}_{\tilde{A}}(x)$ and $\underline{\mu}_{\tilde{A}}(x)$, respectively)

$$\mu_{A_e(l)}(x)=\begin{cases}\bar{\mu}(x) & \text{if } x \leqslant l\\ \underline{\mu}(x) & \text{if } x > l\end{cases} \tag{26}$$

where l is a *switch point*, i.e. the value of x at which $A_e(l)$ switches from $\bar{\mu}(x)$ to $\underline{\mu}(x)$. Then

$$c_l(\widetilde{A})=\min_{l\in X}\text{centroid}(A_e(l)) \tag{27}$$

where

$$\text{centroid}(A_e(l))=\frac{\int_{-\infty}^{l}x\bar{\mu}(x)\,\mathrm{d}x+\int_{l}^{\infty}x\underline{\mu}(x)\,\mathrm{d}x}{\int_{-\infty}^{l}\bar{\mu}(x)\,\mathrm{d}x+\int_{l}^{\infty}\underline{\mu}(x)\,\mathrm{d}x} \tag{28}$$

Similarly, let $A_e(r)$ denote an embedded T1 FS for which

$$\mu_{A_e(r)}(x) = \begin{cases} \underline{\mu}(x) & \text{if } x \leqslant r \\ \bar{\mu}(x) & \text{if } x > r \end{cases} \tag{29}$$

where r is another *switch point*, i.e. the value of x at which $A_e(r)$ switches from $\underline{\mu}(x)$ to $\bar{\mu}(x)$. Then

$$c_r(\widetilde{A}) = \max_{r \in X} \text{centroid}(A_e(r)) \tag{30}$$

where

$$\text{centroid}(A_e(r)) = \frac{\int_{-\infty}^{r} x\underline{\mu}(x)\,dx + \int_{r}^{\infty} x\bar{\mu}(x)\,dx}{\int_{-\infty}^{r} \underline{\mu}(x)\,dx + \int_{r}^{\infty} \bar{\mu}(x)\,dx} \tag{31}$$

4. Properties of the centroid

In this section we provide a collection of properties for the centroid that are valid for any IT2 FS. We use the term "centroid" to mean the centroid of an IT2 FS.

Theorem 1. *The left and right end-points of the centroid, $c_l(\widetilde{A})$ and $c_r(\widetilde{A})$, satisfy the following equations*:

$$c_l(\widetilde{A}) = \frac{\int_{-\infty}^{c_l} x\bar{\mu}(x)\,dx + \int_{c_l}^{\infty} x\underline{\mu}(x)\,dx}{\int_{-\infty}^{c_l} \bar{\mu}(x)\,dx + \int_{c_l}^{\infty} \underline{\mu}(x)\,dx} \tag{32}$$

$$c_r(\widetilde{A}) = \frac{\int_{-\infty}^{c_r} x\underline{\mu}(x)\,dx + \int_{c_r}^{\infty} x\bar{\mu}(x)\,dx}{\int_{-\infty}^{c_r} \underline{\mu}(x)\,dx + \int_{c_r}^{\infty} \bar{\mu}(x)\,dx} \tag{33}$$

Proof. See Appendix B.1. □

The results in (32) and (33) are very interesting and somewhat surprising, in that they show that for $c_l(\widetilde{A})$, when the value of l is found that minimizes centroid$(A_e(l))$ it will be $l = c_l(\widetilde{A})$; and, for $c_r(\widetilde{A})$, when the value of r is found that maximizes centroid$(A_e(r))$ it will be $r = c_r(\widetilde{A})$. Of course, if X is discretized (for computational purposes) then $l \to L \approx c_l(\widetilde{A})$ but L does not exactly equal $c_l(\widetilde{A})$, and $r \to R \approx c_r(\widetilde{A})$ but R does not exactly equal $c_r(\widetilde{A})$, which probably explains why (32) and (33) were not observed by Karnik and Mendel.

Note that the Karnik–Mendel algorithms for finding $c_l(\widetilde{A})$ and $c_r(\widetilde{A})$ are instantiations of (32) and (33), respectively.

Theorem 2. *Let $\widetilde{A}$ be an IT2 FS defined on X, and $\widetilde{A}'$ be $\widetilde{A}$ shifted by*[7] *Δm along X, i.e.*

$$\underline{\mu}_{\widetilde{A}'}(x) = \underline{\mu}_{\widetilde{A}}(x - \Delta m) \tag{34}$$

$$\bar{\mu}_{\widetilde{A}'}(x) = \bar{\mu}_{\widetilde{A}'}(x - \Delta m) \tag{35}$$

Then the centroid of $\widetilde{A}'$, $[c_l(\widetilde{A}'), c_r(\widetilde{A}')]$, is the same as the centroid of $\widetilde{A}$, $[c_l(\widetilde{A}),\ c_r(\widetilde{A})]$, shifted by Δm, i.e.

$$c_l(\widetilde{A}') = c_l(\widetilde{A}) + \Delta m \tag{36}$$

$$c_r(\widetilde{A}') = c_r(\widetilde{A}) + \Delta m \tag{37}$$

Proof. See Appendix B.2. □

Theorem 2 demonstrates that the span of the centroid set of an IT2 FS is *shift-invariant*. This means that regardless of where along X the FOU of $\widetilde{A}$ occurs, as long as the FOU for $\widetilde{A}'$ is unchanged, then

$$\text{span}[\text{centroid}(\widetilde{A}')] = c_r(\widetilde{A}') - c_l(\widetilde{A}') = \text{span}[\text{centroid}(\widetilde{A})] = c_r(\widetilde{A}) - c_l(\widetilde{A}) \tag{38}$$

[7] Δm may be positive or negative.

Theorem 2 also justifies our shifting the FOU of $\widetilde{A}$ to a possibly more convenient point along X for the actual computation of the centroid (e.g., to the origin). When we do that we are computing $c_l(\widetilde{A}')$ and $c_r(\widetilde{A}')$, after which we can compute the centroid of $\widetilde{A}$, using (36) and (37), as $c_l(\widetilde{A}) = c_l(\widetilde{A}') - \Delta m$ and $c_r(\widetilde{A}) = c_r(\widetilde{A}') - \Delta m$.

Theorem 3. (a) *If* $FOU(\widetilde{A})$ *is amplitude scaled by* λ, *where* $0 < \lambda < 1$, *meaning that* $FOU(\widetilde{A}) \to \lambda FOU(\widetilde{A})$ (*i.e.* $\bar{\mu}_{\widetilde{A}'}(x) = \lambda\bar{\mu}_{\widetilde{A}}(x)$ *and* $\underline{\mu}_{\widetilde{A}'}(x) = \lambda\underline{\mu}_{\widetilde{A}}(x)$) *then the centroid is FOU scale-invariant.* (b) *If* $FOU(\widetilde{A})$ *is shifted vertically by a constant amount* (*i.e.* $\bar{\mu}_{\widetilde{A}'}(x) = \bar{\mu}_{\widetilde{A}}(x) + \delta$ *and* $\underline{\mu}_{\widetilde{A}'}(x) = \underline{\mu}_{\widetilde{A}}(x) + \delta$) *then the centroid is not vertically shift-invariant.* (c) *If the primary variable* x *is uniformly scaled to* x/γ, *where* $\gamma > 0$ (*i.e.* $\bar{\mu}_{\widetilde{A}}(x) = \bar{\mu}_{\widetilde{A}}(x/\lambda)$ *and* $\underline{\mu}_{\widetilde{A}'}(x) = \underline{\mu}_{\widetilde{A}}(x/\lambda)$) *then the centroid scales by* γ *to* $\gamma[c_l(\widetilde{A}),\ c_r(\widetilde{A})]$.

Proof. See Appendix B.3. □

Note that if IT2 FS $\widetilde{A}$ is a *normal* FS, then at least one value of its UMF must equal 1. Amplitude scaling and vertical shifting are not permitted if normality must be preserved, in which case Parts (a) and (b) of this theorem are inapplicable to such a normal FS. In Section 6 we will see that a fuzzy granule does not have to be normal, and so scaling of it may be permissible (as long as the UMF of the shifted or scaled FG does not exceed 1).

Theorem 4. *If the primary variable* (x) *is bounded, i.e.* $x \in [x_L, x_R]$, *so that* $x_1 \equiv x_L$ *and* $x_N \equiv x_R$, *then*

$$c_l(\widetilde{A}) \geqslant x_L \tag{39}$$

$$c_r(\widetilde{A}) \leqslant x_R \tag{40}$$

Proof. See Appendix B.4. □

So even though we cannot in general obtain closed-form formulas for the centroid end-points, this theorem provides us with a quick way to check an aspect of computed values for those end-points. Unfortunately, this theorem is not very informative for an IT2 FS that is associated with Gaussian primary MFs, because for such a T2 FS $x_L = -\infty$ and $x_R = \infty$.

Theorem 5. *If* $LMF(\widetilde{A})$ *is entirely on the primary-variable* (x) *axis, and* $x \in [x_L, x_R]$, *then the centroid does not depend upon the shape of* $FOU(\widetilde{A})$ *and, as the sampling approaches zero, it equals* $[x_L, x_R]$.

Proof. See Appendix B.5. □

An example of a FOU for which $\mathrm{LMF}(\widetilde{A})$ is entirely on the primary-variable (x) axis, and $x \in [x_L, x_R]$, is depicted in Fig. 2. It is called a *completely filled-in FOU*. While the results of this theorem may seem strange, let us remember that each of the centroids in (16) that make up the centroid of $\widetilde{A}$ provides a center of gravity about the vertical (primary membership) axis and according to Theorem 4 each of these centroids must be contained within $[x_L, x_R]$. For a completely filled-in FOU, the centroid actually equals $[x_L, x_R]$.

Interval T2 FSs with symmetrical FOUs have been very widely used by practitioners of T2 FSs (e.g., [1,5–10,12,19]). We turn next to such FSs.

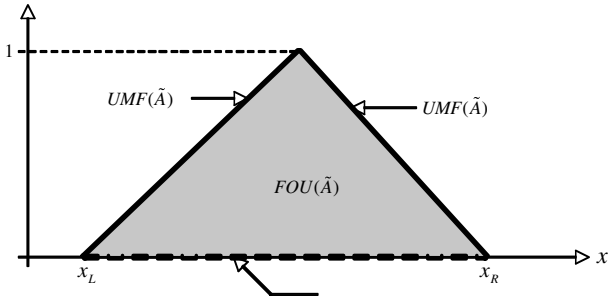

Fig. 2. Completely filled-in FOU.

5. The centroid and its properties for a symmetric FOU

Symmetrical FOUs occur frequently, e.g., create a FOU by starting with a Gaussian primary MF and allow its mean, standard deviation or both to vary over intervals, then the resulting FOU will be symmetrical (e.g., Fig. 4). For such a FOU, we have:

Theorem 6 ([14,15]). *Given a FOU for an IT2 FS, one that is symmetrical about primary variable y at y = m (e.g., Fig. 4), then the centroid of such a T2 FS is symmetrical about y = m, and the average value (i.e. the defuzzified value) of all the elements in the centroid equals m.*

Proof. See Appendix B.6. □

Although the results in this theorem may seem intuitive to some readers, its proof requires some effort. Here (as in [14,15]) we explain the importance of the theorem. First of all, *its results represent a 50% savings in computation for a symmetrical FOU*. Instead of having to compute both $c_l(\widetilde{A})$ and $c_r(\widetilde{A})$, one only needs to compute e.g., $c_l(\widetilde{A})$ using a KM algorithm, after which one can compute $c_r(\widetilde{A})$ from the formula

$$c_r(\widetilde{A}) = 2m - c_l(\widetilde{A}) \tag{41}$$

This equation is a direct result of the symmetry of the centroid about m.

Additionally, suppose we begin with interval T2 fuzzy numbers, each characterized by a symmetrical FOU, and perform an operation (e.g., arithmetic, set-theoretic, non-linear function) on them that leads to another interval T2 fuzzy number that also has a symmetrical FOU, then according to this theorem the result of combined centroid plus defuzzification procedures (which are performed after these operations) could just as well have been obtained by treating the T2 fuzzy numbers as crisp numbers and performing crisp operations on them. In short, *for such T2 fuzzy numbers and operations, if all that is desired is a crisp number after performing said operations on the T2 fuzzy numbers, then it is a waste of effort to perform the calculations using T2 FS mathematics*. All knowledge about the uncertainties of the numbers, as captured by their T2 MFs, is lost at the end of the centroid + defuzzification procedures. Of course, the centroid of such IT2 FSs still provides a useful measure of the uncertainties that have propagated through the operations. These observations lead us to the following:

Corollary 1 (To Theorem 6). *If all that is desired is a crisp number after performing operations on IT2 FSs, then for the use of such sets to make a difference to not using them (e.g., to using T1 FSs or just crisp numbers) the operations that are applied to them must lead to an IT2 FS that has a non-symmetrical FOU.*

Interestingly enough, non-symmetrical FOUs occur in IT2 Mamdani or TSK (Takagi–Sugeno–Kang) rule-based FLSs [12]. For example, in an IT2 Mamdani FLS, although the FOU for each fired rule is usually symmetrical (e.g., Fig. 5) this symmetry is (fortunately) lost when the fired rule T2 FSs are combined, e.g., by

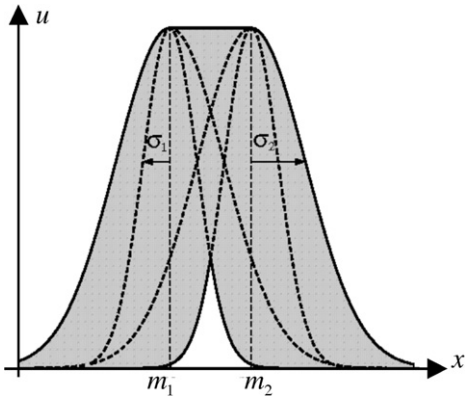

Fig. 4. FOU that is symmetrical about $m = \frac{1}{2}(m_1 + m_2)$.

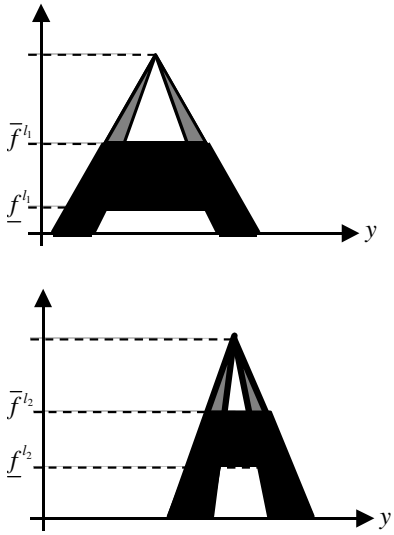

Fig. 5. Fired output sets (dark shaded regions) for two fired rules in an IT2 Mamdani FLS when min t-norm is used.

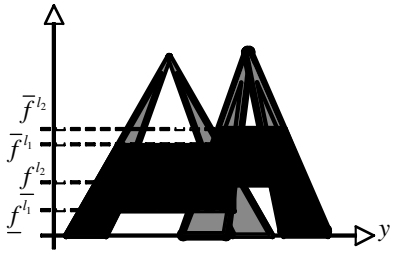

Fig. 6. Union combined output set (dark shaded region) for the two fired output sets in this figure.

union (e.g., Fig. 6), height defuzzification, etc. Note that in Figs. 5 and 6 light shaded regions are the FOUs of two fired consequent sets, $\underline{f}^1$ and $\overline{f}^1$ are the lower and upper firing levels for Rule-1, and $\underline{f}^2$ and $\overline{f}^2$ are the comparable quantities for Rule-2. Formulas for these upper and lower firing levels can be found in [5,12].

Theorem 7. *If the IT2 FS $\widetilde{A}$ defined on X is symmetrical about $m \in X$, then*

$$c_l(\widetilde{A}) \leqslant m \tag{42}$$

$$c_r(\widetilde{A}) \geqslant m \tag{43}$$

Proof. See Appendix B.7. □

This theorem demonstrates that for a symmetrical FOU the centroid end-points cannot crossover to the other side of the symmetry point of the FOU, i.e. c_l must lie to the left of m and c_r must lie to the right of m. A comparable result does not exist for a non-symmetrical FOU.

6. The centroid of an interval type-2 fuzzy granule

A fuzzy granule, introduced by Zadeh (e.g., [23]), often has the shape of a rectangle (Fig. 7). It is interpreted (by us) as the FOU of an IT2 FS, and subsequently as an IT2 FS. In the sequel we shall denote the type-2 fuzzy granule as T2 FG. It is the only IT2 FS (so far) for which we have been able to compute the centroid in closed form. In this section we show some of the details for doing this.

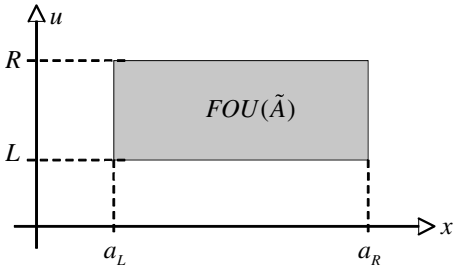

Fig. 7. FOU of an interval T2 fuzzy granule.

Examining Fig. 7, we see that $\underline{\mu}_{\tilde{A}}(x) = L$ and $\bar{\mu}_{\tilde{A}}(x) = R$ for $x \in [a_L, a_R]$; hence, (24) and (25) can be expressed as[8]

$$c_l(\widetilde{A}) = \frac{R\sum_{i=1}^{L^*} x_i + L\sum_{i=L^*+1}^{N} x_i}{\sum_{i=1}^{L^*} R + \sum_{i=L^*+1}^{N} L} \tag{44}$$

$$c_r(\widetilde{A}) = \frac{L\sum_{i=1}^{R^*} x_i + R\sum_{i=R^*+1}^{N} x_i}{\sum_{i=1}^{R^*} L + \sum_{i=R^*+1}^{N} R} \tag{45}$$

where $x_1 = a_L$, $x_N = a_R$ and $x_i = a_L + (i-1)(a_R - a_L)/(N-1)$. As $N \to \infty$ and $x_{i+1} - x_i \to 0$, we can express (44) and (45) in their continuous forms, as

$$c_l(\widetilde{A}) = \frac{R\int_{a_L}^{\alpha_l} x\,\mathrm{d}x + L\int_{\alpha_l}^{a_R} x\,\mathrm{d}x}{R\int_{a_L}^{\alpha_l} \mathrm{d}x + L\int_{\alpha_l}^{a_R} \mathrm{d}x} \tag{46}$$

$$c_r(\widetilde{A}) = \frac{L\int_{a_L}^{\alpha_r} x\,\mathrm{d}x + R\int_{\alpha_r}^{a_R} x\,\mathrm{d}x}{R\int_{a_L}^{\alpha_r} \mathrm{d}x + L\int_{\alpha_r}^{a_R} \mathrm{d}x} \tag{47}$$

where $\alpha_l, \alpha_r \in [a_L, a_R]$ are the switching points for $c_l(\widetilde{A})$ and $c_r(\widetilde{A})$. It is easy to show that (46) and (47) can be expressed as

$$c_l(\widetilde{A}) = \frac{R(\alpha_l + a_L)(\alpha_l - a_L) + L(a_R + \alpha_l)(a_R - \alpha_l)}{2R(\alpha_l - a_L) + 2L(a_R - \alpha_l)} \tag{48}$$

$$c_r(\widetilde{A}) = \frac{L(\alpha_r + a_L)(\alpha_r - a_L) + R(a_R + \alpha_r)(a_R - \alpha_r)}{2L(\alpha_r - a_L) + 2R(a_R - \alpha_r)} \tag{49}$$

Since α_l minimizes $c_l(\widetilde{A})$, the derivative of $c_l(\widetilde{A})$ with respect to α_l must be zero, i.e. $\mathrm{d}c_l/\mathrm{d}\alpha_l = 0$; hence, it follows that

$$\frac{(R-L)\left[(R-L)\alpha_l^2/2 - (Ra_L - La_R)\alpha_l + (Ra_L^2 - La_R^2)/2\right]}{\left[R(\alpha_l - a_L) + L(a_R - \alpha_l)\right]^2} = 0 \tag{50}$$

Letting the numerator of (50) equal zero, we obtain two possible values for α_l, namely

$$\alpha_l = \frac{(Ra_L - La_R) \pm \sqrt{RL}(a_R - a_L)}{R - L} \tag{51}$$

Because $\alpha_l \in [a_L, a_R]$, it is easy to show that only the positive solution in (51) is permissible; hence,

$$\alpha_l = \frac{(Ra_L - La_R) + \sqrt{RL}(a_R - a_L)}{R - L} = \frac{\sqrt{L}a_R + \sqrt{R}a_L}{\sqrt{L} + \sqrt{R}} \tag{52}$$

[8] Because we are using L and R in this section to denote the vertical dimensions of the T2 FG, we use $L*$ and $R*$ in (24) and (25) to denote the two switch points.

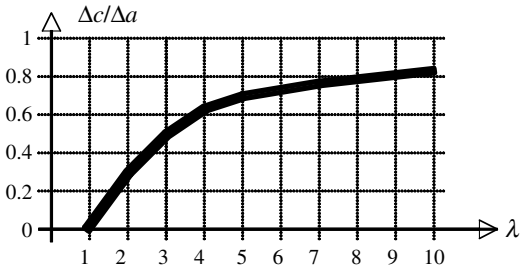

Fig. 8. Uncertainty curve for an IT2 FG.

Substituting (52) into (48), we find (after some algebra) that

$$c_l(\widetilde{A}) = \frac{\sqrt{L}a_R + \sqrt{R}a_L}{\sqrt{L} + \sqrt{R}} \tag{53}$$

Proceeding in a similar manner for $c_r(\widetilde{A})$, by setting $\mathrm{d}c_r/\mathrm{d}\alpha_r = 0$, we find first that

$$\alpha_r = \frac{(Ra_R - La_L) - \sqrt{RL}(a_R - a_L)}{R - L} = \frac{\sqrt{R}a_R + \sqrt{L}a_L}{\sqrt{R} + \sqrt{L}} \tag{54}$$

and then that

$$c_r(\widetilde{A}) = \frac{\sqrt{R}a_R + \sqrt{L}a_L}{\sqrt{R} + \sqrt{L}} \tag{55}$$

Observe, from (52) and (53) that $\alpha_l = c_l(\widetilde{A})$ and from (54) and (55) that $\alpha_r = c_r(\widetilde{A})$, exactly as predicted by Theorem 1; hence, these calculations provide us with additional confirmation of the correctness of the results of that theorem.

Observe, also that

$$c_r(\widetilde{A}) - c_l(\widetilde{A}) = (a_R - a_L)\frac{\sqrt{R} - \sqrt{L}}{\sqrt{R} + \sqrt{L}} = (a_R - a_L)\frac{\sqrt{R/L} - 1}{\sqrt{R/L} + 1} \tag{56}$$

which provides us with the uncertainty interval for a T2 FG as an explicit function of its four defining parameters. Additionally, observe from (56) that:

1. When $L = 0$, $c_r(\widetilde{A}) - c_l(\widetilde{A}) = a_R - a_L$, which is in agreement with Theorem 5, since for the T2 FG (see Fig. 7) $x_1 = a_L$ and $x_N = a_R$.
2. The defuzzified value of the centroid, x_{D}, given by

$$x_{\mathrm{D}} \equiv \frac{c_l(\widetilde{A}) + c_r(\widetilde{A})}{2} = \frac{a_L + a_R}{2} \tag{57}$$

does not depend on the vertical dimensions of the T2 FG, whereas the centroid does; hence, x_{D} is not a useful measure of the uncertainty of a T2 FG, whereas the centroid is.

A plot of (56) is given in Fig. 8. In that figure we have let:

$$\Delta a \equiv a_R - a_L \tag{58}$$

$$\Delta c \equiv c_r - c_l \tag{59}$$

$$\lambda \equiv \sqrt{R/L} \quad \text{and} \quad \lambda > 1 \tag{60}$$

so[9] that (56) can be re-expressed as

$$\Delta c = \Delta a\left(\frac{\lambda-1}{\lambda+1}\right) \tag{61}$$

Observe that as λ increases $\Delta c/\Delta a \to 1$. One way to use Fig. 8 is to specify a value for λ, read off the value of $\Delta c/\Delta a$, fix a value for Δc and compute Δa.

7. Conclusions

In this paper we have collected very useful properties about the centroid of an IT2 FS, and have also illustrated many of the general results for an IT2 fuzzy granule (T2 FG). At present, the T2 FG is the only IT2 FS for which it is possible to obtain closed-form formulas for the centroid.

As mentioned in [17], intuitively we anticipate that geometric properties about the FOU, such as its area and the center of gravities (centroids) of its upper and lower MFs, will be associated with the amount of uncertainty in an IT2 FS. Because closed-form formulas do not exist for c_l and c_r, it is impossible (except for the T2 FG in Section 6) to study how these end-points explicitly depend upon the geometric properties of the FOU. Interestingly enough, upper and lower bounds on c_l and c_r can be expressed in terms of the geometric properties. For derivations of these bounds and discussions on how to use the bounds for solving forward problems (i.e. how to go from parametric IT2 FS models to data) and inverse problems (i.e. how to go from uncertain data to parametric IT2 FS models—*type-2 fuzzistics*), see [17–19].

Appendix A. The Karnik–Mendel (KM) algorithms for determining $c_l(\widetilde{A})$ and $c_r(\widetilde{A})$

A.1. KM algorithm for $c_r(\widetilde{A})$

The five steps of this algorithm are:

1. Initialize θ_i by setting

$$\theta_i = \frac{1}{2}\left[\underline{\mu}_{\widetilde{A}}(x_i) + \bar{\mu}_{\widetilde{A}}(x_i)\right] \quad i = 1,\ldots,N \tag{A.1}$$

and then compute

$$c' = c(\theta_1,\ldots,\theta_N) = \frac{\sum_{i=1}^{N} x_i\theta_i}{\sum_{i=1}^{N}\theta_i} \tag{A.2}$$

2. Find k $(1 \leqslant k \leqslant N-1)$ such that

$$x_k \leqslant c' \leqslant x_{k+1} \tag{A.3}$$

3. Set

$$\theta_i = \begin{cases} \underline{\mu}_{\widetilde{A}}(x_i) & i \leqslant k \\ \bar{\mu}_{\widetilde{A}}(x_i) & i \geqslant k+1 \end{cases} \tag{A.4}$$

and compute

$$c'' = \frac{\sum_{i=1}^{k} x_i\underline{\mu}_{\widetilde{A}}(x_i) + \sum_{i=k+1}^{N} x_i\bar{\mu}_{\widetilde{A}}(x_i)}{\sum_{i=1}^{k}\underline{\mu}_{\widetilde{A}}(x_i) + \sum_{i=k+1}^{N}\bar{\mu}_{\widetilde{A}}(x_i)} \tag{A.5}$$

4. Check if $c'' = c'$. If yes, stop and set $c'' = c_r$. If no, go to Step 5.
5. Set $c' = c''$ and go to Step 2.

[9] $\lambda > 1$ because $R > L$ (see Fig. 7).

A.2. KM algorithm for $c_l(\widetilde{A})$

Same as previous procedure, except in Step 3, set

$$\theta_i = \begin{cases} \bar{\mu}_{\widetilde{A}}(x_i) & i \leqslant k \\ \underline{\mu}_{\widetilde{A}}(x_i) & i \geqslant k+1 \end{cases} \tag{A.6}$$

so that

$$c'' = \frac{\sum_{i=1}^{k} x_i \bar{\mu}_{\widetilde{A}}(x_i) + \sum_{i=k+1}^{N} x_i \underline{\mu}_{\widetilde{A}}(x_i)}{\sum_{i=1}^{k} \bar{\mu}_{\widetilde{A}}(x_i) + \sum_{i=k+1}^{N} \underline{\mu}_{\widetilde{A}}(x_i)} \tag{A.7}$$

Appendix B. Proofs of theorems

B.1. Proof of Theorem 1

We only prove (32) because the proof of (33) is so similar, and we do this in two steps:

- *Step 1*: We show that[10] c_l satisfies the following equation:

$$[\bar{\mu}(c_l) - \underline{\mu}(c_l)]\left\{c_l\left[\int_{-\infty}^{c_l} \bar{\mu}(x)\,\mathrm{d}x + \int_{c_l}^{\infty} \underline{\mu}(x)\,\mathrm{d}x\right] - \left[\int_{-\infty}^{c_l} x\bar{\mu}(x)\,\mathrm{d}x + \int_{c_l}^{\infty} x\underline{\mu}(x)\,\mathrm{d}x\right]\right\} = 0 \tag{B.1}$$

- *Step 2*: We show that c_l can only be as in (32).

Step 1: Beginning with (26)–(28), (27) implies that the derivative of centroid ($A_e(l)$) with respect to l is zero when evaluated at c_l, i.e.

$$\frac{\mathrm{d}}{\mathrm{d}l}\left[\frac{\int_{\infty}^{1} x\bar{\mu}(x) + \int_{l}^{\infty} x\underline{\mu}(x)\,\mathrm{d}x}{\int_{-\infty}^{l} \bar{\mu}(x)\,\mathrm{d}x + \int_{l}^{\infty} \underline{\mu}(x)\,\mathrm{d}x}\right]\Bigg|_{l=c_l} \tag{B.2}$$

This equation expands to

$$\frac{[c_l\bar{\mu}(c_l) - c_l\underline{\mu}(c_l)]\left[\int_{-\infty}^{c_l} \bar{\mu}(x)\,\mathrm{d}x + \int_{c_l}^{\infty} \underline{\mu}(x)\,\mathrm{d}x\right] - [\bar{\mu}(c_l) - \underline{\mu}(c_l)]\left[\int_{-\infty}^{c_l} x\bar{\mu}(x)\,\mathrm{d}x + \int_{c_l}^{\infty} x\underline{\mu}(x)\,\mathrm{d}x\right]}{\left[\int_{-\infty}^{c_l} \bar{\mu}(x)\,\mathrm{d}x + \int_{c_l}^{\infty} \underline{\mu}(x)\,\mathrm{d}x\right]^2} = 0 \tag{B.3}$$

from which it follows that:

$$[\bar{\mu}(c_l) - \underline{\mu}(c_l)]\left\{c_l\left[\int_{-\infty}^{c_l} \bar{\mu}(x)\,\mathrm{d}x + \int_{c_l}^{\infty} \underline{\mu}(x)\,\mathrm{d}x\right] - \left[\int_{-\infty}^{c_l} x\bar{\mu}(x)\,\mathrm{d}x + \int_{c_l}^{\infty} x\underline{\mu}(x)\,\mathrm{d}x\right]\right\} = 0 \tag{B.4}$$

which is (B.1).

Step 2: Let $l_1 \in X$ for which

$$\bar{\mu}(l_1) - \underline{\mu}(l_1) = 0 \tag{B.5}$$

[10] Unless otherwise noted, in this Appendix c_l and c_r are short for $c_l(\widetilde{A})$ and $c_r(\widetilde{A})$.

and $l_2 \in X$ for which

$$l_2\left[\int_{-\infty}^{l_2}\bar{\mu}(x)\,\mathrm{d}x+\int_{l_2}^{\infty}\underline{\mu}(x)\,\mathrm{d}x\right]=\left[\int_{-\infty}^{l_2}x\bar{\mu}(x)\,\mathrm{d}x+\int_{l_2}^{\infty}x\underline{\mu}(x)\,\mathrm{d}x\right] \tag{B.6}$$

Observe that (B.6) can be solved for l_2, and expressed as

$$l_2=\mathrm{centroid}(A_\mathrm{e}(l_2)) \tag{B.7}$$

Since both l_1 and l_2 satisfy (B.1), either or both of them may be c_l. We now show that

$$\mathrm{centroid}(A_\mathrm{e}(l_1))\geqslant\mathrm{centroid}(A_\mathrm{e}(l_2))\quad\text{when } l_1\neq l_2 \tag{B.8}$$

Because c_l is the minimum of the centroids of all embedded T1 FSs, it therefore cannot be centroid $(A_\mathrm{e}(l_1))$, but must be centroid $(A_\mathrm{e}(l_2))$.

If it happens that $l_1=l_2=c_l$, then it may happen that[11] $\bar{\mu}(c_l)=\underline{\mu}(c_l)$, in which case (B.1) is simultaneously satisfied by *both* of its terms equaling zero. By these arguments we see that (B.1) can never be satisfied by $\bar{\mu}(c_l)=\underline{\mu}(c_l)$ alone.

Returning to the proof of (B.8), we first consider the case when $l_1<l_2$, for which centroid $(A_\mathrm{e}(l_1))$ can be re-expressed as

$$\begin{aligned}\mathrm{centroid}(A_\mathrm{e}(l_1))&=\frac{\int_{-\infty}^{l_1}x\bar{\mu}(x)\,\mathrm{d}x+\int_{l_1}^{\infty}x\underline{\mu}(x)\,\mathrm{d}x}{\int_{-\infty}^{l_1}\bar{\mu}(x)\,\mathrm{d}x+\int_{l_1}^{\infty}\underline{\mu}(x)\,\mathrm{d}x}\\&=\frac{\int_{-\infty}^{l_2}x\bar{\mu}(x)\,\mathrm{d}x-\int_{l_1}^{l_2}x\bar{\mu}(x)\,\mathrm{d}x+\int_{l_2}^{\infty}x\underline{\mu}(x)\,\mathrm{d}x+\int_{l_1}^{l_2}x\underline{\mu}(x)\,\mathrm{d}x}{\int_{-\infty}^{l_2}\bar{\mu}(x)\,\mathrm{d}x-\int_{l_1}^{l_2}\bar{\mu}(x)\,\mathrm{d}x+\int_{l_2}^{\infty}\underline{\mu}(x)\,\mathrm{d}x+\int_{l_1}^{l_2}\underline{\mu}(x)\,\mathrm{d}x}\\&=\frac{\int_{-\infty}^{l_2}x\bar{\mu}(x)\,\mathrm{d}x+\int_{l_2}^{\infty}x\underline{\mu}(x)\,\mathrm{d}x-\int_{l_1}^{l_2}x[\bar{\mu}(x)-\underline{\mu}(x)]\,\mathrm{d}x}{\int_{-\infty}^{l_2}\bar{\mu}(x)\,\mathrm{d}x+\int_{l_2}^{\infty}\underline{\mu}(x)\,\mathrm{d}x-\int_{l_1}^{l_2}[\bar{\mu}(x)-\underline{\mu}(x)]\,\mathrm{d}x}\\&=\frac{l_2\left[\int_{-\infty}^{l_2}\bar{\mu}(x)\,\mathrm{d}x+\int_{l_2}^{\infty}\underline{\mu}(x)\,\mathrm{d}x\right]-\int_{l_1}^{l_2}x[\bar{\mu}(x)-\underline{\mu}(x)]\,\mathrm{d}x}{\int_{-\infty}^{l_2}\bar{\mu}(x)\,\mathrm{d}x+\int_{l_2}^{\infty}\underline{\mu}(x)\,\mathrm{d}x-\int_{l_1}^{l_2}[\bar{\mu}(x)-\underline{\mu}(x)]\,\mathrm{d}x}\end{aligned} \tag{B.9}$$

In obtaining this last line, we have substituted the left-hand side of (B.6) for the right-hand side of (B.6), where the latter appears in the numerator of the third line of (B.9). Because $l_2>l_1$ and it is always true that $\bar{\mu}(x)-\underline{\mu}(x)\geqslant 0$, it follows that:

$$0<\int_{l_1}^{l_2}x[\bar{\mu}(x)-\underline{\mu}(x)]\,\mathrm{d}x\leqslant l_2\int_{l_1}^{l_2}[\bar{\mu}(x)-\underline{\mu}(x)]\,\mathrm{d}x \tag{B.10}$$

Upon the substitution of the upper bound in (B.10) into the numerator of (B.9), we see that

$$\mathrm{centroid}(A_\mathrm{e}(l_1))\geqslant\frac{l_2\left[\int_{-\infty}^{l_2}\bar{\mu}(x)\,\mathrm{d}x+\int_{l_2}^{\infty}\underline{\mu}(x)\,\mathrm{d}x\right]-l_2\int_{l_2}^{l_1}[\bar{\mu}(x)-\underline{\mu}(x)]\,\mathrm{d}x}{\int_{-\infty}^{l_2}\bar{\mu}(x)\,\mathrm{d}x+\int_{l_2}^{\infty}\underline{\mu}(x)\,\mathrm{d}x-\int_{l_2}^{l_1}[\bar{\mu}(x)-\underline{\mu}(x)]\,\mathrm{d}x}\geqslant l_2=\mathrm{centroid}(A_\mathrm{e}(l_2)) \tag{B.11}$$

where the last part of (B.11) follows from (B.7). This completes the proof of (B.8) when $l_1<l_2$.

[11] The condition $\bar{\mu}(c_l)=\underline{\mu}(c_l)$ means that at $x=c_l$ the upper and lower MFs touch each other, something that is perfectly permissible in the FOU$(\tilde{A})$.

Turning next to the case when $l_1 > l_2$, we see that centroid $(A_e(l_1))$ can be re-expressed as

$$\begin{aligned}
\text{centroid}(A_e(l_1)) &= \frac{\int_{-\infty}^{l_1} x\bar{\mu}(x)\,dx + \int_{l_1}^{\infty} x\underline{\mu}(x)\,dx}{\int_{-\infty}^{l_1} \bar{\mu}(x)\,dx + \int_{l_1}^{\infty} \underline{\mu}(x)\,dx} \\
&= \frac{\int_{-\infty}^{l_2} x\bar{\mu}(x)\,dx + \int_{l_2}^{l_1} x\bar{\mu}(x)\,dx + \int_{l_2}^{\infty} x\underline{\mu}(x)\,dx - \int_{l_2}^{l_1} x\underline{\mu}(x)\,dx}{\int_{-\infty}^{l_2} \bar{\mu}(x)\,dx + \int_{l_2}^{l_1} \bar{\mu}(x)\,dx + \int_{l_2}^{\infty} \underline{\mu}(x)\,dx - \int_{l_2}^{l_1} \underline{\mu}(x)\,dx} \\
&= \frac{\int_{-\infty}^{l_2} x\bar{\mu}(x)\,dx + \int_{l_2}^{\infty} x\underline{\mu}(x)\,dx + \int_{l_2}^{l_1} x[\bar{\mu}(x) - \underline{\mu}(x)]\,dx}{\int_{-\infty}^{l_2} \bar{\mu}(x)\,dx + \int_{l_2}^{\infty} \underline{\mu}(x)\,dx + \int_{l_2}^{l_1} [\bar{\mu}(x) - \underline{\mu}(x)]\,dx} \\
&= \frac{l_2\left[\int_{-\infty}^{l_2} \bar{\mu}(x)\,dx + \int_{l_2}^{\infty} \underline{\mu}(x)\,dx\right] + \int_{l_2}^{l_1} x[\bar{\mu}(x) - \underline{\mu}(x)]\,dx}{\int_{-\infty}^{l_2} \bar{\mu}(x)\,dx + \int_{l_2}^{\infty} \underline{\mu}(x)\,dx + \int_{l_2}^{l_1} [\bar{\mu}(x) - \underline{\mu}(x)]\,dx}
\end{aligned} \tag{B.12}$$

In obtaining this last line, we have substituted the left-hand side of (B.6) for the right-hand side of (B.6), where the latter appears in the numerator of the third line of (B.12). Because $l_1 > l_2$, and it is always true that $\bar{\mu}(x) - \underline{\mu}(x) \geqslant 0$, it follows that:

$$\int_{l_2}^{l_1} x[\bar{\mu}(x) - \underline{\mu}(x)]\,dx \geqslant l_2 \int_{l_2}^{l_1} [\bar{\mu}(x) - \underline{\mu}(x)]\,dx \tag{B.13}$$

Upon the substitution of (B.13) into the numerator of (B.12), we see that

$$\text{centroid}(A_e(l_1)) \geqslant \frac{l_2\left[\int_{-\infty}^{l_2} \bar{\mu}(x)\,dx + \int_{l_2}^{\infty} \underline{\mu}(x)\,dx\right] + l_2 \int_{l_2}^{l_1} [\bar{\mu}(x) - \underline{\mu}(x)]\,dx}{\int_{-\infty}^{l_2} \bar{\mu}(x)\,dx + \int_{l_2}^{\infty} \underline{\mu}(x)\,dx + \int_{l_2}^{l_1} [\bar{\mu}(x) - \underline{\mu}(x)]\,dx} \geqslant l_2 = \text{centroid}(A_e(l_2)) \tag{B.14}$$

which proves (B.8) when $l_1 > l_2$.

Eqs. (B.11) and (B.14) together prove the truth of (B.8). Consequently, it is only l_2 that is the legitimate solution of (B.1), and therefore $l_2 = c_l$, where c_l is given by (32).

B.2. Proof of Theorem 2

We only prove (36) because the proof of (37) is so similar. Eqs. (26)–(28) are for fuzzy set $\widetilde{A}$. Their comparable equations for fuzzy set $\widetilde{A}'$ are

$$\mu_{A'_e(l)}(x) = \begin{cases} \bar{\mu}_{\widetilde{A}'}(x) & \text{if } x \leqslant l \\ \underline{\mu}_{\widetilde{A}'}(x) & \text{if } x > l \end{cases} \tag{B.15}$$

$$c_l(\widetilde{A}') = \min_{l \in X} \text{centroid}(A'_e(l)) \tag{B.16}$$

$$\text{centroid}(A'_e(l)) = \frac{\int_{-\infty}^{l} x\bar{\mu}_{\widetilde{A}'}(x)\,dx + \int_{l}^{\infty} x\underline{\mu}_{\widetilde{A}'}(x)\,dx}{\int_{-\infty}^{l} \bar{\mu}_{\widetilde{A}'}(x)\,dx + \int_{l}^{\infty} \underline{\mu}_{\widetilde{A}'}(x)\,dx} \tag{B.17}$$

Substituting (34) and (35) into (B.17), we find that

$$\begin{aligned}
\text{centroid}(A'_e(l)) &= \frac{\int_{-\infty}^{l} x\bar{\mu}_{\widetilde{A}}(x - \Delta m)\,dx + \int_{l}^{\infty} x\underline{\mu}_{\widetilde{A}}(x - \Delta m)\,dx}{\int_{-\infty}^{l} \bar{\mu}_{\widetilde{A}}(x - \Delta m)\,dx + \int_{l}^{\infty} \underline{\mu}_{\widetilde{A}}(x - \Delta m)\,dx} \\
&= \frac{\int_{-\infty}^{l} (x - \Delta m)\bar{\mu}_{\widetilde{A}}(x - \Delta m)\,dx + \int_{l}^{\infty} (x - \Delta m)\underline{\mu}_{\widetilde{A}}(x - \Delta m)\,dx}{\int_{-\infty}^{l} \bar{\mu}_{\widetilde{A}}(x - \Delta m)\,dx + \int_{l}^{\infty} \underline{\mu}_{\widetilde{A}}(x - \Delta m)\,dx} + \Delta m \\
&= \frac{\int_{-\infty}^{l-\Delta m} y\bar{\mu}_{\widetilde{A}}(y)\,dy + \int_{l-\Delta m}^{\infty} y\underline{\mu}_{\widetilde{A}}(y)\,dy}{\int_{-\infty}^{l-\Delta m} \bar{\mu}_{\widetilde{A}}(y)\,dy + \int_{l-\Delta m}^{\infty} \underline{\mu}_{\widetilde{A}}(y)\,dy} + \Delta m = \text{centroid}(A_e(l - \Delta m)) + \Delta m
\end{aligned} \tag{B.18}$$

Substituting (B.18) into (B.16), it follows that (note that X' is the domain for A'_e, and X is the domain for A_e, where $X' = X - \Delta m$):

$$\begin{aligned} c_l(\widetilde{A}') &= \min_{l\in X'} \text{centroid}(A'_e(l)) = \Delta m + \min_{l\in X'} \text{centroid}(A_e(l-\Delta m)) = \Delta m + \min_{t\in X} \text{centroid}(A_e(t)) \\ &= \Delta m + c_l(\widetilde{A}) \end{aligned} \tag{B.19}$$

which is (36).

B.3. Proof of Theorem 3

(a) Amplitude scaling $\text{FOU}(\widetilde{A})$ by λ means that $\text{FOU}(\widetilde{A}) \to \lambda FOU(\widetilde{A})$, where $0 < \lambda < 1$, [in which case $\text{UMF}(\widetilde{A}) \to \lambda UMF(\widetilde{A})$ and $\text{LMF}(\widetilde{A}) \to \lambda \text{LMF}(\widetilde{A})$] so that:

$$\frac{\sum_{i=1}^N x_i\theta_i}{\sum_{i=1}^N \theta_i} \to \frac{\sum_{i=1}^N x_i\lambda\theta_i}{\sum_{i=1}^N \lambda\theta_i} = \frac{\sum_{i=1}^N x_i\theta_i}{\sum_{i=1}^N \theta_i} \tag{B.20}$$

Because scale factor λ cancels from the numerator and denominator, (17) and (18) are unchanged when $\text{FOU}(\widetilde{A})$ is scaled by λ, and we say that the centroid is *FOU scale-invariant*.

(b) Shifting $\text{FOU}(\widetilde{A})$ vertically by a constant amount, say v, we see that:

$$\frac{\sum_{i=1}^N x_i\theta_i}{\sum_{i=1}^N \theta_i} \to \frac{\sum_{i=1}^N x_i(\theta_i + v)}{\sum_{i=1}^N (\theta_i + v)} \neq \frac{\sum_{i=1}^N x_i\theta_i}{\sum_{i=1}^N \theta_i} \tag{B.21}$$

hence, (17) and (18) change when $\text{FOU}(\widetilde{A})$ is shifted vertically by a constant amount. This means that the centroid is *not* vertically shift-invariant.

(c) Note that in our notation θ_i is short for $\theta_i(x_i)$. Let $\widetilde{A}'$ denote the scaled version of $\widetilde{A}$, for which the MF of every embedded T1 FS is $\mu_{A'_e}(x) = \mu_{A_e}(x/\gamma)$. Then

$$\text{Centroid}(A'_e) = \frac{\sum_{i=1}^N x_i\theta_i(x_i/\gamma)}{\sum_{i=1}^N \theta_i(x_i/\gamma)} = \gamma\frac{\sum_{i=1}^N \frac{x_i}{\gamma}\theta_i(x_i/\gamma)}{\sum_{i=1}^N \theta_i(x_i/\gamma)} = \gamma\frac{\sum_{i=1}^N y_i\theta_i(y_i)}{\sum_{i=1}^N \theta_i(y_i)} = \gamma\text{Centroid}(A_e) \tag{B.22}$$

So all of the centroids of all embedded T1 FSs are scaled by γ; hence, by virtue of (17) and (18), and $\gamma > 0$,

$$[c_l, c_r] \to \gamma[c_l, c_r] \tag{B.23}$$

which means that centroid $[c_l, c_r]$ is scaled by γ.

B.4. Proof of Theorem 4

That $c_l \geqslant x_L$ follows from:

$$\frac{\sum_{i=1}^N x_i\theta_i}{\sum_{i=1}^N \theta_i} \geqslant x_1\frac{\sum_{i=1}^N \theta_i}{\sum_{i=1}^N \theta_i} = x_1 \equiv x_L \tag{B.24}$$

which is (39). That $c_r \leqslant x_R$ follows from:

$$\frac{\sum_{i=1}^N x_i\theta_i}{\sum_{i=1}^N \theta_i} \leqslant x_N\frac{\sum_{i=1}^N \theta_i}{\sum_{i=1}^N \theta_i} = x_N \equiv x_R \tag{B.25}$$

which is (40).

B.5. Proof of Theorem 5

To show $c_l = x_L$ consider the embedded T1 FS (see Fig. 3) $\{(x_L,0),(x_2,\varepsilon),(x_3,0),\ldots,(x_R,0)\}$. When $\varepsilon \to 0$ the sampling approaches zero, and $x_2 \to x_L$. It follows that:

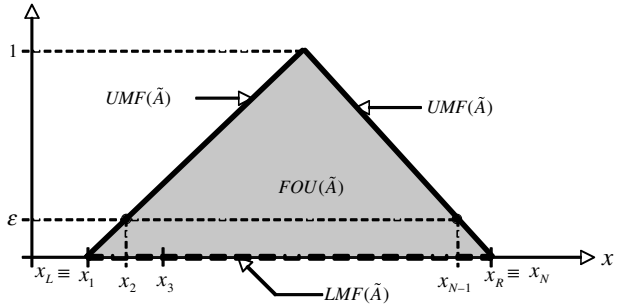

Fig. 3. Constructions for the two embedded T1 FSs that are used in the proof of Theorem 5.

$$\frac{\sum_{i=1}^{N} x_i\theta_i}{\sum_{i=1}^{N}\theta_i} = \frac{x_2\varepsilon}{\varepsilon} = x_2 \to x_L \quad \text{as } \varepsilon \to 0 \tag{B.26}$$

From Theorem 4, we know that $c_l \geqslant x_L$; hence, this fact together with (B.26) let us conclude that $c_l = x_L$.

To show $c_r = x_R$, consider the embedded T1 FS (see Fig. 3) $\{(x_L,0),(x_2,0),\ldots,(x_{N-1},\varepsilon),(x_R,0)\}$. When $\varepsilon \to 0$ the sampling approaches zero, and $x_{N-1} \to x_R$. It follows that:

$$\frac{\sum_{i=1}^{N} x_i\theta_i}{\sum_{i=1}^{N}\theta_i} = \frac{x_{N-1}\varepsilon}{\varepsilon} = x_{N-1} \to x_R \quad \text{as } \varepsilon \to 0 \tag{B.27}$$

From Theorem 4, we know that $c_r \leqslant x_R$; hence, this fact together with (B.27) let us conclude that$c_r = x_R$.

B.6. Proof of Theorem 6

A complete proof of this theorem appears in [15]. It relies very heavily on the Mendel–John Representation Theorem, and the facts that:

1. For an origin-shifted symmetrical FOU, all of its embedded T2 FSs are either symmetrical about $y = 0$ or are unsymmetrical about $y = 0$.
2. For an origin-shifted symmetrical FOU, all of the symmetrical embedded T2 FSs have a centroid equal to[12] 1/0.
3. For an origin-shifted symmetrical FOU, all of the unsymmetrical embedded T2 FSs occur as pairs of mirror images about the vertical axis.
4. Let $g(y)$ denote an origin-shifted unsymmetrical embedded T2 FS with centroid $1/\bar{g}$, and $h(y)$ denote the mirror image of $g(y)$ with centroid $1/\bar{h}$. Then, $1/\bar{h} = 1/-\bar{g}$.

B.7. Proof of Theorem 7

Let $\widetilde{A}'$ denote $\widetilde{A}$ shifted to the origin, so that in Theorem 2, $\Delta m = -m$. We first prove that $c_l(\widetilde{A}') \leqslant 0$ when $\widetilde{A}'$ is symmetrical about the origin. Having done that, then from Theorem 2, it will be true that $c_l(\widetilde{A}) = c_l(\widetilde{A}') + m \leqslant m$.

Consider a special embedded T1 FS A'_e, defined as

$$\mu_{A'_e}(x) = \begin{cases} \bar{\mu}(x) & \text{if } x \leqslant 0 \\ \underline{\mu}(x) & \text{if } x > 0 \end{cases} \tag{B.28}$$

[12] 1/0 is the T2 representation of 0, i.e. it is 0 *for sure*, so that the secondary grade of 0 is 1.

The centroid of A'_e is

$$\text{centroid}(A'_e) = \frac{\int_{-\infty}^{0} x\bar{\mu}(x)\,dx + \int_{0}^{\infty} x\underline{\mu}(x)\,dx}{\int_{-\infty}^{0} \bar{\mu}(x)\,dx + \int_{0}^{\infty} \underline{\mu}(x)\,dx} = \frac{\int_{0}^{\infty} -x\bar{\mu}(-x)\,dx + \int_{0}^{\infty} x\underline{\mu}(x)\,dx}{\int_{0}^{\infty} \bar{\mu}(-x)\,dx + \int_{0}^{\infty} \underline{\mu}(x)\,dx} \tag{B.29}$$

Making use of the symmetry of $\widetilde{A}'$ about the origin [(9) and (10) in which $m = 0$], we find that:

$$\text{centroid}(A'_e) = \frac{-\int_{0}^{\infty} x[\bar{\mu}(x) - \underline{\mu}(x)]\,dx}{\int_{0}^{\infty} \bar{\mu}(x)\,dx + \int_{0}^{\infty} \underline{\mu}(x)\,dx} \leqslant 0 \tag{B.30}$$

because $\bar{\mu}(x) \geqslant \underline{\mu}(x)$ for $\forall x \in X$. Since $c_l(\widetilde{A}')$ must be at least as small as $\text{centroid}(A'_e)$, we have therefore shown that $c_l(\widetilde{A}') \leqslant 0$.

The proof that $c_r(\widetilde{A}') \geqslant m$ is so similar to the proof that $c_l(\widetilde{A}) \leqslant m$, we leave it to the reader.

References

[1] H. Hagras, A hierarchical type-2 fuzzy logic control architecture for autonomous mobile robots, IEEE Trans. Fuzzy Syst. 12 (August) (2004) 524–539.
[2] C. Hwang, F. Rhee, An interval type-2 fuzzy spherical shells algorithm, in: Proc. IEEE Int. Conf. Fuzzy Systems, Budapest, Hungary, July 2004.
[3] N.N. Karnik, J.M. Mendel, An introduction to type-2 fuzzy logic systems, USC Report, University of Southern Calif., 1998.
[4] N.N. Karnik, J.M. Mendel, Centroid of a type-2 fuzzy set, Inf. Sci. 132 (2001) 195–220.
[5] Q. Liang, J.M. Mendel, Interval type-2 fuzzy logic systems: theory and design, IEEE Trans. Fuzzy Syst. 8 (October) (2000) 535–550.
[6] Q. Liang, J.M. Mendel, Equalization of nonlinear time-varying channels using type-2 fuzzy adaptive filters, IEEE Trans. Fuzzy Syst. 8 (October) (2000) 551–563.
[7] Q. Liang, J.M. Mendel, Overcoming time-varying co-channel interference using type-2 fuzzy adaptive filter, IEEE Trans. Circ. Syst. 47 (December) (2000) 1419–1428.
[8] Q. Liang, J.M. Mendel, Designing interval type-2 fuzzy logic systems using an SVD–QR method: rule reduction, Int. J. Intell. Syst. 15 (2000) 939–957.
[9] Q. Liang, J.M. Mendel, Modeling MPEG VBR video traffic using type-2 fuzzy logic systems, in: W. Pedrycz (Ed.), Granular Computing an Emerging Paradigm, Physica-Verlag, New York, 2000, pp. 367–383.
[10] Q. Liang, N.N. Karnik, J.M. Mendel, Connection admission control in ATM networks using survey-based type-2 fuzzy logic systems, IEEE Trans. Syst., Man Cyber. Part C: Appl. Rev. 30 (August) (2000) 329–339.
[11] T.-S. Liou, M.-J.J. Wang, Fuzzy weighted average: an improved algorithm, Fuzzy Sets Syst. 49 (1992) 307–315.
[12] J.M. Mendel, Uncertain Rule-Based Fuzzy Logic Systems: Introduction and New Directions, Prentice-Hall, Upper Saddle River, NJ, 2001.
[13] J.M. Mendel, On the importance of interval sets in type-2 fuzzy logic systems, in: Proc. Joint 9th IFSA World Congress and 20th NAFIPS Int'l. Conf., Vancouver, British Columbia, Canada, 2001, pp. 1647–1652.
[14] J.M. Mendel, Centroid and defuzzified value of an interval type-2 fuzzy set whose footprint of uncertainty is symmetrical, in: Proc. IPMU, Perugia, Italy, July 2004.
[15] J.M. Mendel, On a 50% savings in the computation of the centroid of a symmetrical interval type-2 fuzzy set, Inf. Sci. 172 (2005) 417–430.
[16] J.M. Mendel, R.I. Bob John, Type-2 fuzzy sets made simple, IEEE Trans. Fuzzy Syst. 10 (April) (2002) 117–127.
[17] J.M. Mendel, H. Wu, Centroid uncertainty bounds for interval type-2 fuzzy sets: forward and inverse problems, in: Proc. IEEE Int'l. Conf. Fuzzy Syst., Budapest, Hungary, 2004.
[18] J.M. Mendel, H. Wu, Type-2 fuzzistics for symmetric interval type-2 fuzzy sets: Part 1, forward problems, IEEE Trans. Fuzzy Syst., in press.
[19] J.M. Mendel, H. Wu, Type-2 fuzzistics for symmetric interval type-2 fuzzy sets: Part 2, inverse problems, IEEE Trans. on Fuzzy Syst., in press.
[20] J. Starczewski, L. Rutkowski, Interval type-2 neuro-fuzzy systems based on interval consequents, in: Proc. 6th Int'l. Conf. Neural Networks and Soft Computing: Studies on Fuzziness and Soft Computing, Physica-Verlag, Heidelberg, 2003, pp. 570–577.
[21] H. Wu, J.M. Mendel, Uncertainty bounds and their use in the design of interval type-2 fuzzy logic systems, IEEE Trans. Fuzzy Syst. 10 (October) (2002) 622–639.
[22] K.C. Wu, Fuzzy interval control of mobile robots, Comput. Electr. Eng. 22 (1996) 211–229.
[23] L.A. Zadeh, Toward a theory of fuzzy information granulation and its centrality in human reasoning and fuzzy logic, Fuzzy Sets Syst. 90 (1997) 111–137.